Science of the Total Environment 772 (2021) 145386

Contents lists available at ScienceDirect

Science of the Total Environment

journal homepage: www.elsevier.com/locate/scitotenv

The relationships of present vegetation, bacteria, and soil properties with soil organic matter characteristics in moist acidic tundra in Alaska

Sungjin Nam [a,1], Josu G. Alday [b,c,1], Mincheol Kim [a], Hyemin Kim [a,2], Yongkang Kim [d], Taesung Park [d], Hyoun Soo Lim [e], Bang Yong Lee [a], Yoo Kyung Lee [a,*], Ji Young Jung [a,*]

[a] Korea Polar Research Institute, Incheon 21990, Republic of Korea
[b] Joint Research Unit CTFC - AGROTECNIO, Av. Alcalde Rovira Roure 191, E25198 Lleida, Spain
[c] Department of Crop and Forest Sciences, University of Lleida, Av. Alcalde Rovira Roure 191, E25198 Lleida, Spain
[d] Department of Statistics, Seoul National University, Seoul 08826, Republic of Korea
[e] Department of Geological Sciences, Pusan National University, Busan 46241, Republic of Korea

HIGHLIGHTS

- SOM composition, vegetation, bacteria, and soil traits were simultaneously examined.
- SOM composition was spatially structured and partially related to elevation.
- There was no direct vegetation effect on SOM composition variation.
- Soil traits and bacterial composition mostly explained SOM compositional variation.
- Soil pH, moisture, and carbon content were related to SOM composition.

GRAPHICAL ABSTRACT

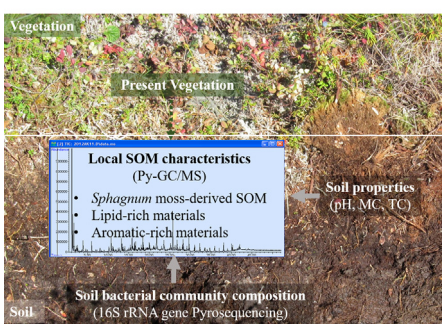

ARTICLE INFO

Article history:
Received 6 October 2020
Received in revised form 19 January 2021
Accepted 19 January 2021
Available online 27 January 2021

Editor: Manuel Esteban Lucas-Borja

Keywords:
Soil organic matter (SOM)
Sphagnum moss
Soil properties
Microbiome
Moist acidic tundra
Pyrolysis GC/MS

ABSTRACT

Soil organic matter (SOM) is related to vegetation, soil bacteria, and soil properties; however, not many studies link all these parameters simultaneously, particularly in tundra ecosystems vulnerable to climate change. Our aim was to describe the relationships between vegetation, bacteria, soil properties, and SOM composition in moist acidic tundra by integrating physical, chemical, and molecular methods. A total of 70 soil samples were collected at two different depths from 36 spots systematically arranged over an area of about 300 m × 50 m. Pyrolysis-gas chromatography/mass spectrometry and pyrosequencing of the 16S rRNA gene were used to identify the molecular compositions of the SOM and bacterial community, respectively. Vegetation and soil physicochemical properties were also measured. The sampling sites were grouped into three, based on their SOM compositions: *Sphagnum* moss-derived SOM, lipid-rich materials, and aromatic-rich materials. Our results show that SOM composition is spatially structured and linked to microtopography; however, the vegetation, soil properties, and bacterial community composition did not show overall spatial structuring. Simultaneously, soil properties and bacterial community composition were the main factors explaining SOM compositional variation, while vegetation had a residual effect. Verrucomicrobia and Acidobacteria were related to polysaccharides, and Chloroflexi was linked to aromatic compounds. These relationships were consistent across different hierarchical levels. Our results suggest

* Corresponding authors.
E-mail addresses: yklee@kopri.re.kr (Y.K. Lee), jyjung@kopri.re.kr (J.Y. Jung).
[1] These authors contributed equally to this work. They should be considered as co-first authors.
[2] Present address: Mediogen, 120, Bio valley 1-ro, Jecheon-si, Chungcheongbuk-do 27159, Republic of Korea.

https://doi.org/10.1016/j.scitotenv.2021.145386

that SOM composition at a local scale is closely linked with soil factors and the bacterial community. Comprehensive observation of ecosystem components is recommended to understand the in-situ function of bacteria and the fate of SOM in the moist acidic tundra.

1. Introduction

Soil is the largest carbon reservoir in the terrestrial ecosystem, and thus small changes in soil carbon might greatly affect the carbon balance in the ecosystem (Lal, 2004; Schuur et al., 2008; Schmidt et al., 2011). Recently, Arctic permafrost has gained much attention owing to global warming, because its vast amount of preserved soil organic matter (SOM) is vulnerable to climate change (Schuur et al., 2008). A recent estimation of the soil organic carbon (SOC) pool in the Northern Hemisphere permafrost was approximately 1035 Pg carbon in the top 3 m of soil (Hugelius et al., 2014). Warming would cause permafrost thawing and active layer deepening, thus leading to increases in greenhouse gas emissions into the atmosphere through microbial processes (Karhu et al., 2014). This could result in strong positive feedback to climate change (Davidson and Janssens, 2006; Schuur et al., 2009).

The composition of SOM is generally described by the chemistry of plant inputs, as a major source material. It is well known that vegetation-derived compounds appear in SOM compositions (Vancampenhout et al., 2010; Stewart et al., 2011) and that SOM composition varies following vegetation changes (Guo et al., 2016). Plant chemistry strongly affects chemical composition of SOM in most natural systems. However, there are other source materials for SOM formation, such as microbial-derived compounds which have not been studied very well. For example, soil microbes degrade plants inputs and synthesize various substances, contributing to chemically diverse and stable SOM formation (Kallenbach et al., 2016). Microbial decomposition changes the litter/SOM chemistry, which affects microbial community structure and turnover (Moorhead and Sinsabaugh, 2006; Kallenbach et al., 2016). Despite the importance of soil microbial roles in SOM formation and decomposition, only a limited number of studies have investigated the links between SOM composition and soil microbial communities simultaneously.

In addition to vegetation and soil microbes, there are numerous reports showing close relationships between environmental parameters and SOC content, stocks, or turnover (Post and Kwon, 2000; Meersmans et al., 2008); however, relatively fewer studies have focused on the relationships between these abiotic factors and SOM composition. For example, SOM characteristics have been compared among agricultural practices including tillage and mulching (Ding et al., 2002; De la Rosa et al., 2019), air temperatures, land uses (Pisani et al., 2016), and fire histories and restoration managements (Jimenez-Gonzalez et al., 2016; López-Martin et al., 2016; Jimenez-Morillo et al., 2020). However, there are several studies showing that multiple factors interact with SOM. Wang et al. (2016) reported that temperature, rainfall, soil order, landscape, and land-use could explain the variability of SOM composition after conducting SOM analysis across a wide range of grasslands in New Zealand. Vancampenhout et al. (2010) also examined several soil variables controlling SOM composition, including dominant vegetation. Thus, soil environmental variables should be considered to clearly understand the multidimensional nature of SOM composition.

Pyrolysis-gas chromatography/mass spectrometry (Py-GC/MS) has been widely used to characterize SOM composition at a molecular level (Buurman et al., 2007; Vancampenhout et al., 2010; Derenne and Tu, 2014). Pyrolysis uses high temperatures to degrade complicated compounds into small fragments, which can then be easily analyzed. The mixture of small fragments is separated by gas chromatography (GC), and then each component is identified by mass spectrometry (MS). Py-GC/MS allows rapid analysis of overall SOM composition because it does not require any pre-treatment, extraction, or derivatization, and the runtime of GC is relatively short (Mehrabanian, 2013). Py-GC/MS identifies specific SOM compounds, rather than simply showing chemical functional groups like spectroscopic methods, e.g. Fourier-transform infrared and NMR spectroscopy (Derenne and Tu, 2014; Derenne and Quenea, 2015). However, this method is still limited when exploring the original structure of SOM, as the thermal reactions can result in secondary modifications and only GC-amenable compounds are detectable (Saiz-jimenez, 1994; Kögel-Knabner, 2000; Derenne and Quenea, 2015; Klein et al., 2020). Nevertheless, it is a powerful tool for assessing the molecular composition of SOM and its biochemical sources.

To date, most research on SOM characteristics has been conducted on a large scale, such as comparisons among different ecosystem types and land uses. For example, Vancampenhout et al. (2009) assessed differences in SOM composition in different climate zones (tundra, taiga, temperate forest, and tropical forest). In Alaska, Treat et al. (2014) compared SOM chemistry between boreal black spruce peatland and tundra peatland. In addition, Dai et al. (2002) explored the bioavailability and chemical composition of SOM from five different Arctic soils. These large-scale approaches can provide insight into ecosystem differences in SOM composition; however, there are many other environmental parameters that co-vary with SOM chemical composition. Thus, SOM composition studies at a local level could more satisfactorily describe these influencing factors by eliminating confounding parameters.

In this paper, we examine SOM chemical composition and its relationships with plant, bacteria, and soil properties in the acidic moist tussock tundra in Council, Alaska. We used a local scale approach to minimize the number of co-varying environmental parameters, such as temperature and precipitation (Vancampenhout et al., 2009). Thus, we characterized the SOM composition of 36 upper and 34 lower soil samples using Py-GC/MS, as well as their vegetation composition, soil properties, and bacterial community composition. The main aim was to describe the molecular composition of SOM at a local scale, as well as the relationships between SOM composition and several biotic and abiotic factors, such as vegetation, bacterial community, and soil physicochemical properties. Specifically, we tested the following hypotheses: (1) there is spatial variability to SOM composition, vegetation, bacterial community composition, and edaphic variables at a local scale, (2) vegetation and bacterial community could be the most influencing factor to SOM compositional variation in upper and lower layers, respectively, and (3) SOM composition shows close relationships with vegetation, soil properties, and bacterial community. To test these hypotheses, we applied a set of multivariate statistics using plant coverage, bacterial community composition, and soil physical and chemical properties data, alongside SOM composition data.

2. Materials and methods

2.1. Study site

The study site, Council (64.51°N, 163.39°W), northeast of Nome on the Seward Peninsula in Alaska, is located in a sub-Arctic transitional region between boreal forest and tundra. The annual average air temperature and annual precipitation recorded at the Nome airport (64.50°N, 165.43°W, 1971 to 2010) are -2.8 ± 1.4 °C and 404.1 ± 93.5 mm, respectively (https://www.ncdc.noaa.gov/cdo-web/). The vegetation is

mainly dominated by moss (*Sphagnum spp.*), cotton grass (*Eriophorum vaginatum*), and bog blueberry (*Vaccinium uliginosum*), which are representatives of the moist acidic tussock tundra (Park and Lee, 2014). Our study site was composed of 25% tussock and 75% inter-tussock, and the soil was classified as Typic Histoturbels in the USDA system and Histic Turbic Cryosols in the WRB system. Thick organic layer was developed on the soil surface.

2.2. Soil sampling and analyses

The soil samples were collected at 36 points arranged in a regular grid, 25 m apart, covering an area of 300 m × 50 m in mid-August. A total of 70 soil samples were collected from two depths (0–10 cm and 10–20 cm) after removing non-decomposed dead plant materials (Oi), except for two points in the lower layer which were skipped owing to the high water table. The soil samples were stored at −20 °C until analysis. The frozen soil was air-dried and sieved through a 2-mm mesh for further SOM analysis. The soil less than 2 mm in size was ground into fine powder.

Before soil sampling, the coverage of each plant species in a 40 × 40 cm quadrat over each sampling site was described. The soil physical and chemical properties and bacterial community composition data used for further data analysis were acquired from Kim et al. (2014), and the experimental methods are described in detail in that publication. Briefly, soil moisture content (MC) was determined by the weight difference between fresh soil and soil dried at 105 °C for 48 h. Soil pH was measured in a soil:water (1:10) solution. The total carbon (TC) and nitrogen (TN) content were determined by combustion at 950 °C (FlashEA 1112; Thermo Fisher Scientific, USA). The inorganic nitrogen content in the soil was analyzed using an Auto-Analyzer (QuAAtro-4ch; Seal Analytical GmbH, Germany) from 2 M KCl soil extracts. The dissolved organic carbon content was determined using a TOC analyzer (TOC_L series, Shimadzu, Japan) from soil filtrates (1:5 soil:water solution).

2.3. Bacterial community analyses

For bacterial community analysis, soil DNA was extracted from 0.5 g of soil samples using a FastDNA® SPIN kit for soil (MP Biomedicals) following the manufacturer's instructions. Extracted DNA was amplified using barcoded fusion primers (27F: 5′- X-AC-AGAGTTTGATCMTGGCTCAG-3′, and 519R: 5′-X-AC-GWATTACCGCGGCKGCTG −3′, where 'X' and 'AC' represent 8 bp barcode and 2 bp linker sequences, respectively) targeting the V1-V3 region of the bacterial 16S rRNA gene. 16S rRNA gene amplicon sequencing data generated by 454 GS FLX Titanium was downloaded from NCBI SRA (SRP026166) (Kim et al., 2014) and processed following the 454 SOP in mothur v.1.44.0 (Schloss et al., 2009). Flowgrams were denoised using the mothur-implemented Pyronoise algorithm and denoised sequences were aligned against the SILVA pre-aligned reference DB (release 128). De novo UCHIME chimera detection algorithm was used to identify putative chimeras. The quality-filtered sequences were clustered into operational taxonomic units (OTUs) with a 97% similarity cutoff with opticlust option, and taxonomically classified against EzBioCloud 16S DB (Yoon et al., 2017) using the naïve Bayesian Classifier with a confidence threshold of 80%. 16S sequences belonging to chloroplasts, mitochondria, or eukaryotes were removed.

2.4. Pyrolysis-gas chromatography/mass spectrometry

The molecular chemical compositions of the SOM samples were analyzed by Py-GC/MS. The fine, powdered soil, wrapped in pyrofoil (Japan Analytical Industry, Tokyo, Japan), was pyrolyzed for 5 s in a quartz tube with a Curie temperature of 590 °C. Curie-point pyrolysis was performed using a Curie-point Injector (Japan Analytical Industry, Tokyo, Japan). The products of pyrolysis were transferred immediately to a GC/MS system, an Agilent 7890A GC equipped with a DB-5ms capillary column (30 m × 250 μm internal diameter × 0.25 μm film thickness) and an Agilent 5975C MS as a detector. The sample was injected with a split ratio of 1:10. Helium was used as a carrier gas with a flow rate of 1 ml min^{-1}. The injector temperature was set to 250 °C. The initial oven temperature was set to 40 °C for 5 min, and then increased to 300 °C at a rate of 7 °C min^{-1}. The final temperature was maintained for 10 min. Electron impact ionization was used, with an ionization energy of 70 eV.

2.5. Data processing of Py-GC/MS

After deconvolution and extraction using AMDIS v. 2.66, each peak was identified by comparing it to the reference spectra of the National Institute of Standards and Technology 2008 (NIST 08) mass library. Peaks present in the first 3 min of retention time were removed to avoid the initial flush of volatile compounds. The 288 pyrolysates (products of pyrolysis) were reduced into 167 components by removing the compounds that were present only in a few samples (less than five) and that had a relative intensity less than 0.1% at the largest. The peak components in each sample were summed and the relative abundance of each pyrolysate was recalculated. The identification and quantification of all individual peaks were carefully checked manually. Among the 167 remaining pyrolysates, 24 products were not identified in the mass library or were not characterized according to their origin and chemical similarity. With reference to previously published literature, a total of 143 pyrolysates were assigned to six categories, according to their origins and chemical similarity: polysaccharides (Ps), lipids (Li), lignin (Lg), nitrogen compounds (N), phenols (Ph), and aromatics (Ar) (Chefetz et al., 2002; Gleixner et al., 2002; Buurman et al., 2007; González-Pérez et al., 2007; Grandy et al., 2009; Mambelli et al., 2011; Stewart, 2012; Schellekens et al., 2017; Chen et al., 2018).

2.6. Statistics

Statistical analyses were performed in the R software environment (v.3.6; R Core Team, 2020), using the vegan package for multivariate and diversity analyses (Oksanen et al., 2019). As sampling site 17 showed completely different SOM characteristics from the rest of the sites, we excluded it in most of the data analyses. While the soil in site 17 showed a silty mineral layer under a thinner organic layer, the other soil samples included a very thick organic horizon. Our study area was located on a wide flood plain developed on alluvium. The soil surface undulated slightly, perhaps caused by thermokarst formation and overland flow during high water scouring (personal communication, Dr. Chien-Lu Ping). This might be the reason for the unique SOM characteristics of site 17 (Fig. S1).

First, a principal component analysis (PCA) was performed to identify which characteristics best grouped the different sampling sites with the 123 and 125 pyrolysis products in upper and lower layers, respectively excluding compounds found only from site 17. Second, we tested if there was any significant spatial structuring in the data matrix (i.e., in the vegetation, bacteria, environmental variables, or SOM characteristic data) before using the data in the subsequent analyses. The spatial distribution of the sampling sites was evaluated using the principal component neighbor matrices method (PCNM; Oksanen et al., 2019). Subsequently, we tested the existence of implicit spatial structure in each matrix of variables using the "capscale" function. Third, we used a variation partitioning approach to disentangle the relative importance of the soil properties, vegetation composition, and spatial effects (PCNMs) as predictors of SOM composition variability. We determined the significance of exclusive and shared effects using a partial redundancy analysis with adjusted canonical R^2 values (Legendre and Legendre, 2012). Fourth, we applied a non-metric multidimensional scaling (NMDS) to the vegetation compositional data to characterize compositional differences between the sampled sites. Over this vegetation ordination, we defined four vegetation clusters based on similarity, using the unweighted pair-groups method using arithmetic averages

Table 1
A list of compounds identified from all 70 samples. The source is the compound code, and each compound was identified using retention time (RT), molecular weight (MW), and major ions.

Source	Compound name	RT	MW	Major ions
Ps1	Isopropyl acetate	3.056	102	43, 61
Ps2	2-Methylfuran	3.592	82	53, 82
Ps3	Glycol, monoacetate	4.031	104	43, 74
Ps4	2(5H)-furanone	4.890	84	54, 84
Ps5	3-Furaldehyde	5.448	96	95, 96
Ps6	2-Furaldehyde [furfural]	5.977	96	95, 96
Ps7	2-Cyclopentene-1,4-dione	6.251	96	42, 96
Ps8	Furan, 2-propyl	7.191	110	91, 110
Ps9	2-Propanone, 1-hydroxy-, acetate	7.334	116	43, 86
Ps10	2-Cyclopenten-1-one, x-methyl	8.418	96	67, 96
Ps11	Furan, 2-acetyl	8.590	110	95, 110
Ps12	2-Cyclopenten-1-one, 2-hydroxy	9.027	98	55, 98
Ps13	2-Furaldehyde, 5-methyl	10.160	110	109, 110
Ps14	2-Cylcolpenten-1-one, x-methyl	10.201	96	67, 96
Ps15	2H-pyran-2,6(3H)-dione	11.054	112	55, 112
Ps16	2-Cyclopenten-1-one, 2-hydroxy-3-methyl	11.884	112	112
Ps17	2,5-Furandicarboxaldehyde	13.326	124	123, 124
Ps18	3(2H)-furanone, 2,5-dimethyl-4-hydroxy	13.459	128	43, 57, 72, 128
Ps19	Benzofuran, 2-methyl	14.010	132	131,132
Ps20	Levoglucosenone	14.041	126	68, 69
Ps21	4H-Pyran-4-one, 3-hydroxy-2-methyl [maltol]	14.056	126	76, 126
Ps22	4H-Pyran-4-one, 2,3-dihydro-3,5,-dihydroxy-6-methyl	14.839	144	101, 144
Ps23	Sugar compound	15.449		60, 73
Ps24	1,4:3,6-Dianhydro-alpha-D-glucopyranose	16.395	144	57, 69
Ps25	Furfural, 5-hydroxymethyl	16.687	126	97, 126
Ps26	Sugar compound	19.610		60, 73
Ps27	D-Allose	20.988	180	60, 73
Ps28	D-Glucopyranose, 1,6-anhydro	21.809	162	60, 73
N1	Pyrrole	3.500	67	67
N2	C1-pyrrole	6.207	81	80, 81
N3	Benzonitrile	10.837	103	76, 103
N4	Pyridinone, 4-amino-2(1H)	10.842	110	82, 110
N5	N-butyl-tert-butylamine	11.245	129	58, 114
N6	Pyrrolidine, 1-ethyl-2,2-dimethyl	11.631	127	84, 112
N7	Benzyl nitrile	14.746	117	90, 117
N8	4-Methyl-2-oxopentanenitrile	15.833	111	41, 43
N9	Indole	18.076	117	90, 117
N10	Indole, 3-methyl	19.897	131	130, 131
N11	3-Pyridinol, 6-methyl-, acetate	20.007	151	80, 109
N12	Diketodipyrrole	25.399	186	93, 186
Ar1	Toluene	3.862	92	91, 92
Ar2	Ethylbenzene	6.930	106	91, 106
Ar3	Dimethylbenzene/p-xylene	7.245	106	91, 106
Ar4	Dimethylbenzene/p-xylene	7.250	106	91, 106
Ar5	Styrene	7.963	104	78, 104
Ar6	Dimethylbenzene/p-xylene	7.974	106	91, 106
Ar7	Benzene, propyl	9.887	120	91, 120
Ar8	Benzene, 1-ethyl-x-methyl	10.113	120	105, 120
Ar9	Benzene, 1-ethyl-x-methyl	10.227	120	105, 120
Ar10	Benzene, 1-ethyl-x-methyl	10.593	120	105, 120
Ar11	Benzene, 1,2,4-trimethyl	11.046	120	105, 120
Ar12	Benzene, 1,2,3-trimethyl	11.776	120	105, 120
Ar13	Indane	12.114	118	117, 118
Ar14	Indene	12.382	116	115, 116
Ar15	Benzeneacetaldehyde	12.445	120	91
Ar16	Indane, 1-methyl	13.411	132	117, 132
Ar17	Benzene, 1-methyl-2-cyclopropen-1-yl	14.924	130	115, 130
Ar18	Indene, 2-methyl	15.111	130	115, 130
Ar19	Naphthalene	15.774	128	128
Ar20	1,2-Benzenediol	16.011	110	64, 110
Ar21	Naphthalene, 2-methyl	18.157	142	115, 142
Ar22	Benzene, 1,2-dicarboxylic acid	18.425	166	76, 104
Ar23	Naphthalene, 1-methyl	18.441	142	141, 142
Ar24	Biphenyl	19.801	154	76, 154
Ar25	Naphthalene, 2-ethyl	20.044	156	141, 156
Ar26	Naphthalene, x,x-dimethyl	20.509	156	141, 156
Ar27	Dibenzofuran	22.327	168	139, 168
Ar28	Fluorene	23.470	166	165, 166
Ar29	9H-fluorene, 9-methylene	26.665	178	176, 178
Ph1	Phenol	10.720	94	66, 94
Ph2	Phenol, 2-methyl	12.677	108	107, 108
Ph3	Phenol, 4-methyl	13.214	108	107, 108
Ph4	Phenol, x-ethyl	14.642	122	107, 122
Ph5	Phenol, 2,4-dimethyl	14.948	122	107, 122
Ph6	Phenol, 4-ethyl	15.351	122	107, 122
Ph7	Phenol, 4-isopropenyl	18.252	134	119, 134
Lg1	Phenol, 2-methoxy [guaiacol]	13.463	124	109, 124
Lg2	Phenol, 4-methyl-2-methoxy [4-methylguaiacol]	15.866	138	123, 138
Lg3	Phenol, 4-vinyl	16.515	120	91, 120
Lg4	Phenol, 4-ethyl-2-methoxy [4-ethylguaiacol]	17.662	152	137, 152
Lg5	Phenol, 4-vinyl-2-methoxy [4-vinylguaiacol]	18.416	150	135, 150
Lg6	Phenol, 5-methyl-3-methoxy	18.611	138	138
Lg7	Vanilin	20.094	152	151, 152
Lg8	Phenol, 2-methoxy-4-(1-propenyl) [isoeugenol]	21.035	164	164
Lg9	Ethanone, 1-(x-hydroxy-x-methoxyphenyl)	21.671	166	151, 166
Lg10	Ethanone, 1-(2,5-dimethoxyphenyl)-[2,5-Dimethoxyacetophenon]	22.997	180	165, 180
Lg11	Phenol, 2,6-dimethoxy-4-(2-propenyl) [methoxyeugenol]	25.272	194	91, 194
Li1	C8:0 [octane]	4.832	114	57, 71
Li2	C9:0 [nonane]	8.307	128	57, 71
Li3	C10:0 [decane]	11.286	142	57, 71
Li4	C11:0 [undecane]	13.838	156	57, 71
Li5	C12:0 [dodecane]	16.111	170	57, 71
Li6	C13:0 [tridecane]	18.197	184	57, 71
Li7	C14:0 [tetradecane]	20.123	198	57, 71
Li8	C15:0 [pentadecane]	21.943	212	57, 71
Li9	C16:0 [hexadecane]	23.665	226	57, 71
Li10	C17:0 [heptadecane]	25.296	240	57, 71
Li11	C18:0 [octadecane]	26.846	254	57, 71
Li12	C19:0 [nonadecane]	28.317	268	57, 71
Li13	C20:0 [eicosane]	29.723	282	57, 71
Li14	C21:0 [heneicosane]	31.059	296	57, 71
Li15	C22:0 [docosane]	32.359	310	57, 71
Li16	C23:0 [tricosane]	33.596	324	57, 71
Li17	C24:0 [tetracosane]	34.786	338	57, 71
Li18	C25:0 [pentacosane]	35.919	352	57, 71
Li19	C27:0 [heptacosane]	38.072	380	57, 71
Li20	C29:0 [nonacosane]	40.088	408	57, 71
Li21	C30:0 [triacontane]	41.973	422	57, 71
Li22	n-C8:1	4.571	112	55, 69
Li23	n-C9:1	8.023	126	55, 69
Li24	n-C10:1	11.043	140	55, 69
Li25	n-C12:1	15.936	168	55, 69
Li26	n-C13:1	18.036	182	55, 69
Li27	n-C14:1	19.987	196	55, 69
Li28	n-C15:1	21.819	210	55, 69
Li29	n-C16:1	23.538	224	55, 69
Li30	n-C17:1	25.183	238	55, 69
Li31	n-C18:1	26.741	252	55, 69
Li32	n-C19:1	28.220	266	55, 69
Li33	n-C20:1	29.635	280	55, 69
Li34	n-C21:1	30.991	294	55, 69
Li35	n-C22:1	32.285	308	55, 69
Li36	n-C23:1	33.531	322	55, 69
Li37	n-C24:1	34.722	336	55, 69
Li38	n-C25:1	35.840	350	55, 69
Li39	n-C26:1	36.972	364	55, 69
Li40	n-C27:1	38.044	378	55, 69
Li41	n-C28:1	39.063	392	55, 69
Li42	Fa(C7) [heptanoic acid]	13.389	130	60, 73
Li43	FA(C8) [octanoic acid]	15.519	144	60, 73
Li44	FA(C16) [hexadecanoic acid]	29.147	256	60, 73
Li45	Stigmastan-3,5-dien	41.832	396	147, 207, 396
Li46	Cholest-5-en-3-one, 22,25-dihydroxy-	44.099	416	207, 414
Li47	Stigmasta-3,5-dien-7-one	45.236	410	174, 410
Li48	Prist-1-ene	25.718	266	55, 69
Li49	Pentadecanal	27.106	226	57, 69
Li50	2-Pentadecanone, 6,10,14-trimethyl	27.458	268	58, 71
Li51	1-Hexadecanol	28.050	242	55, 69
Li52	2-Nonadecanone	31.118	282	58, 71
Li53	1-Eicosanol	33.447	298	55, 83
Li54	Squalene	39.211	410	69, 81
Li55	C27:0 methylketone	40.211	394	58, 59
Li56	C28:0 methylketone	42.164	408	58, 59

Ps: polysaccharides; N: N-containing compounds; Lg: lignins; Ph: phenols; Ar: aromatics; Li: lipids.

(UPGMA) method and Ward distance. We also described the relationships between vegetation composition and soil parameters using the envfit and adonis functions (Oksanen et al., 2019). Then, we evaluated the correlation between SOM composition and vegetation group. Fifth, the relationships between SOM and soil properties were tested using adonis in overall and for each upper and lower layer independently, and the significant soil factors described by adonis were plotted in a PCA ordination of SOM composition for each upper and lower layer independently. Sixth, we evaluated the correlation between SOM composition and bacterial community composition in the upper and lower layers using the Mantel test.

3. Results

3.1. Molecular composition of SOM

A total of 143 pyrolysis products were identified in this study, and their sources are listed in Table 1. Polysaccharides were the most dominant group in the upper layer samples (Table S1). The polysaccharide groups mainly included furans and sugar units which were largely identified as the pyrolysis products of hemicellulose and cellulose (Lv and Wu, 2012). Lipids were the major components in the lower layer (Table S1). The pyrolysates derived from lipids included n-alkanes (C_8–C_{30}; Li1–21), n-alkenes (C_8–C_{28}; Li22–41), fatty acids (Li42–44), sterols (Li45–47), a pristene (Li48), *n*-alcohols (Li49–53), a terpene (Li54), and methylketones (Li55–56). Among the 11 lignin-derived products, 4-vinylphenol (Lg3) and 4-vinylguaiacol (Lg5) were the most abundant compounds (0.4–2%), pyrolytic products of ferulic acid and *p*-coumaric acid, respectively. Among the 12 identified N-compounds (1.0–21.7%), 4-methyl-2-oxo-pentanenitrile and N-butyl-tert-butylamine were major compounds in the pyrogram. The N-containing pyrolysis products included pyrrols, pyridines, and indoles. Phenol (Ph1) and 2/4-methylphenol (Ph2, Ph3) were the most abundant phenol compounds. We also found 4-isopropenylphenol (Ph7) in 17 soil samples. Toluene (Ar1) was the most abundant aromatic compound (1.7–14.3% of total ion current, TIC), followed by ethylbenzene (Ar2), dimethylbenzene (Ar3, Ar6), and styrene (Ar5). The proportion of polyaromatics was extremely low in this study site. The proportions of naphthalene, methylnaphthalene, dimethylnaphthalene, and fluorene were similar, all less than 1% of TIC, except in the lower layer of site 17.

The PCA of the pyrolysis products in the upper layers showed that PC1 and 2 explained 29.6% and 12.2% of the variation, respectively (Fig. 1a). The polysaccharide- and lipid-derived compounds were clearly separated along PC1 (Fig. 1c); the polysaccharides were on the negative side, while the lipids were on the positive side of PC1. Most of the aromatic and phenolic compounds were located on the negative side of PC2, and only one phenolic compound, 4-isopropenylphenol (Ph7), was situated in the middle of the polysaccharide-derived compounds. The lignin-derived compounds were located on the positive side of PC1. The N-containing compounds were scattered throughout the loading plot. For the lower layer samples, PC1 and 2 explained 30.8% and 11.3% of the variation, respectively (Fig. 1b). Overall, the distribution of the pyrolysis products in the lower layer was similar to that in the upper layer; polysaccharides on the left, lipids on the right, and aromatics in the lower half of the plot (Fig. 1d). Although the distribution of hydrocarbons (n-alkanes/n-alkenes) in the upper layer did not show any particular trends, long-chain and short/mid-chain hydrocarbons were separated along PC2 in the lower layer plot. The long-chain hydrocarbons were located on the positive side of PC2, whereas the short/mid-chain hydrocarbons were on the negative side (Fig. 1d).

3.2. Spatial variability of SOM composition, vegetation, bacterial community composition, and soil variables

The preliminary spatial analyses of the data matrices showed a lack of spatial variability in the vegetation, the bacterial community composition in the upper layer, and the soil physicochemical properties (non-significant PCNM axes; $p > 0.05$). In contrast, the SOM composition in both layers and the bacterial community in the lower layer showed significant spatial structuring, with notable similarities

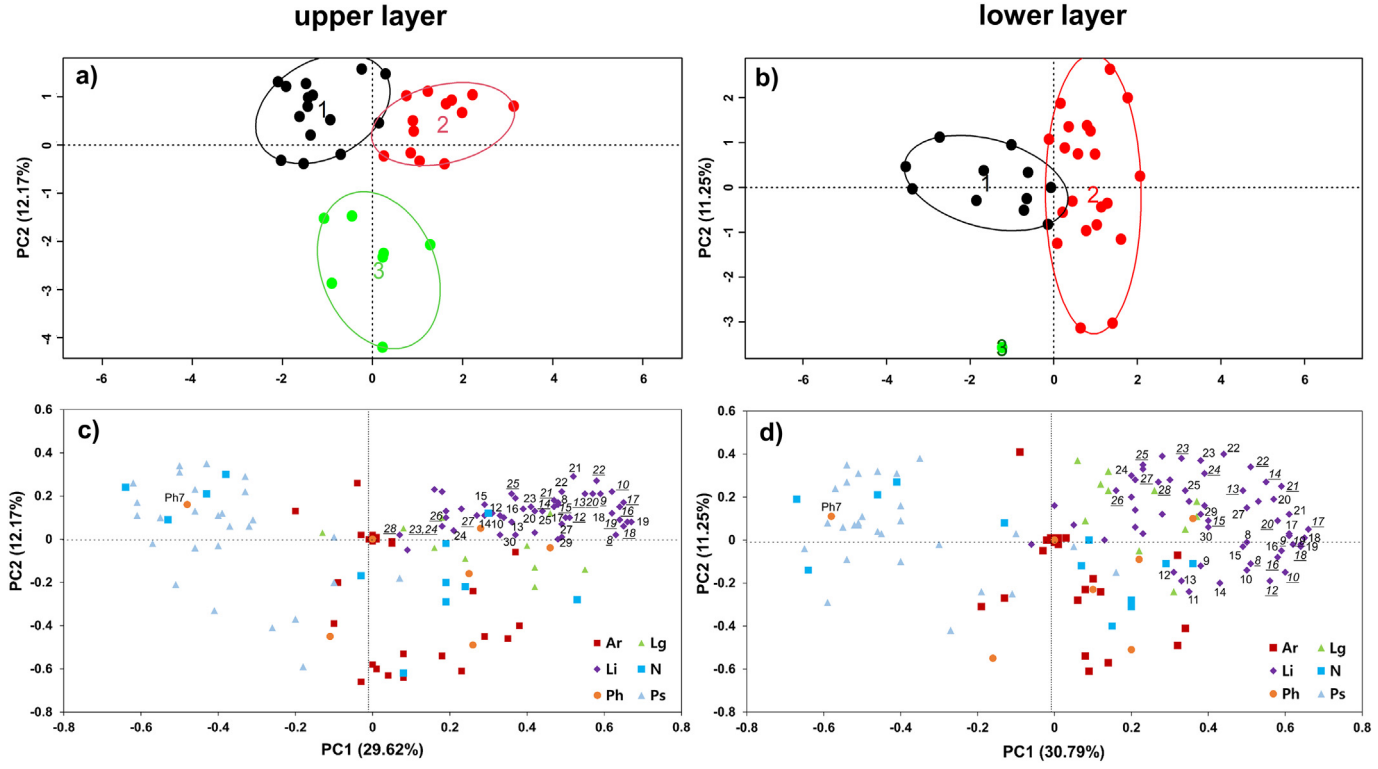

Fig. 1. Principal component analysis (PCA) results using the relative abundances of pyrolysis products in the upper (a, c) and lower soil layers (b, d). The numbers of score plots are the sampling points. Ps: polysaccharides; N: N-containing compounds; Lg: lignins; Ph: phenols; Ar: aromatics; Li: lipids.

between the three matrices (significant PCNM 1, 3, and 4 for SOM composition and 3, 4, and 5 for bacterial community; $p < 0.05$). The underlying spatial variability for the three significant matrices showed that the main differences were produced when comparing the right-hand side sampling sites with the left-hand ones (Fig. S2), mainly because the sites on the right-hand side showed more spatial heterogeneity in their SOM compositions in both layers, and in their bacterial communities in the lower layer, than the left-hand side sites (which were more homogeneous). This spatial trend was significantly related to elevation ($F_{[1,33]} = 2.49$, p-value $= 0.016$), especially PCNM 4, suggesting that the upper layer on the right-hand side of the sampling site had some spatial differences from the rest of the sampling sites.

3.3. Factors influencing SOM composition variation

Considering the SOM composition in the upper layer (Fig. 2a), 35% of the variance was significantly explained by vegetation, soil properties, and spatial components ($p < 0.05$). The main significant influential factors were soil properties (20% pure and 13% shared variation), followed by spatial variation, which accounted for only 14% of the total variance (5% pure spatial component and 9% shared with soil properties and vegetation). In contrast, vegetation did not significantly influence SOM composition in the upper layer directly (only 1% pure component), but it accounted for 13% of the shared variation with soil properties and spatial components. However, when the effects of the bacterial community were considered, a higher proportion of variance was explained (54%). The soil properties and spatial components explained similar proportions of the variation as they did in the previous analyses (Fig. 2a), while the bacterial community significantly explained a 32% of the total variance in SOM composition in the upper layer (20% pure and 12% shared variation with soil properties and spatial components).

When the analysis was repeated for the lower layer (Fig. 2b), 24% of the variance was significantly explained by the soil properties, spatial distance, and vegetation components ($p < 0.05$). The soil properties were the main influential factor, accounting for 23% of the variance (10% pure soil and 13% shared with vegetation and spatial components). The pure effect of the spatial components only represented 2% of the variance, while vegetation composition had no pure effect on SOM composition in the lower layer (all shared variation). When the effects of the bacterial community composition in the lower layer were included, a little more of the variance in SOM composition was explained (30%). The soil properties and spatial components maintained similar explanatory powers, regardless of whether the vegetation or bacterial community composition was considered. However, the bacterial community composition explained 18% of the SOM compositional variation in the lower layer (4% pure bacterial and 14% shared with soil properties and

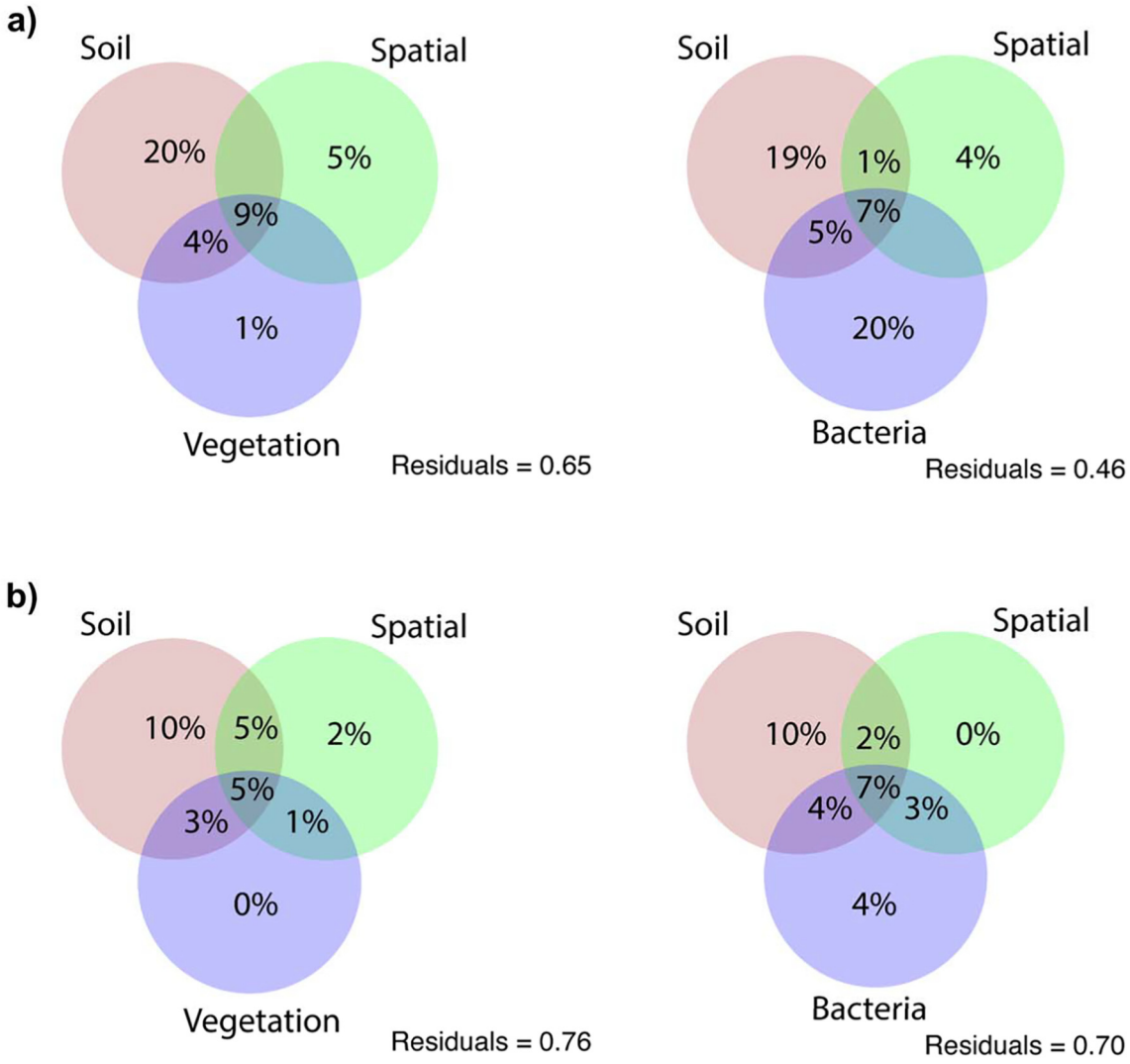

Fig. 2. Variation partitioning analyses for SOM composition including soil properties, spatial distance, and vegetation and bacterial community composition in the (a) upper and (b) lower layers. Values show the fraction of variation explained by each component, as well as the shared contribution of each component.

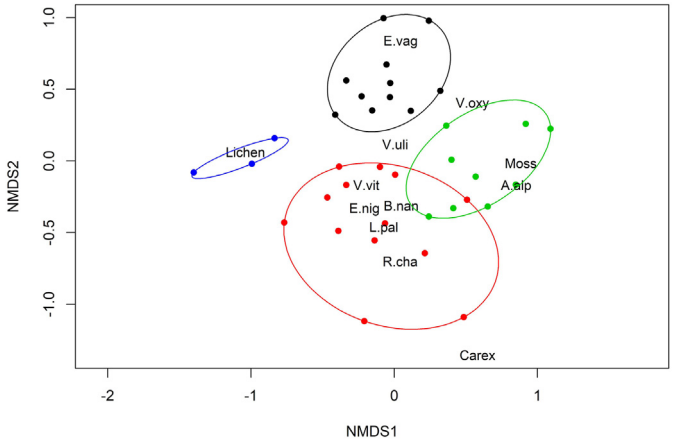

Fig. 3. Non-metric multidimensional scaling (NMDS) of the vegetation compositional data for the Council, AK site. The color sd-ellipses represent each of the vegetation groups described. The species characteristics of these groups are *Eriophorum vaginatum* (E.vag) for G1 (black), lichen for G2 (blue), mosses (*Sphagnum* spp.) for G3 (green), and *Betula nana* (B.nan), *Rubus chamaemorus* (R.cha), *Carex* spp. for G4 (red). (For interpretation of the references to color in this figure legend, the reader is referred to the web version of this article.)

spatial components). The bacterial community composition explained nearly half of the total variation in SOM composition in the lower layer.

3.4. Are there any relationships between vegetation and either SOM composition or soil properties?

The cluster analysis over the NMDS ordination clearly showed four different vegetation communities, characterized by *Eriophorum vaginatum* (G1), lichen (G2), mosses (G3), and *Betula nana*, *Rubus chamaemorus*, and *Carex* spp. (G4), located in different regions of the ordination space (Fig. 3). However, these vegetation groups were not related to any change in soil properties in the upper or lower layers ($p > 0.05$ for all comparisons). Similarly, when the correlation between overall vegetation and SOM composition was tested, no clear relationships were found for either layer (mantel test r-statistic $= -0.02$, p-values $= 0.560$). In addition, when testing if the vegetation groups showed differences in SOM composition using Permutational Multivariate Analysis of Variance, we observed that there were no significant differences in SOM composition between the vegetation groups in either soil layer (upper layer $F_{[3,34]} = 0.69$, p-value $= 0.934$; lower layer $F_{[3,32]} = 1.49$, p-value $= 0.055$). It is clear from the variation partitioning results that there were only marginal or indirect relationships between vegetation composition and SOM composition in both layers.

3.5. Are there any relationships between SOM composition and soil properties?

The soil physicochemical properties were the main source of SOM composition variation, explaining 33% and 23% of the variation in the

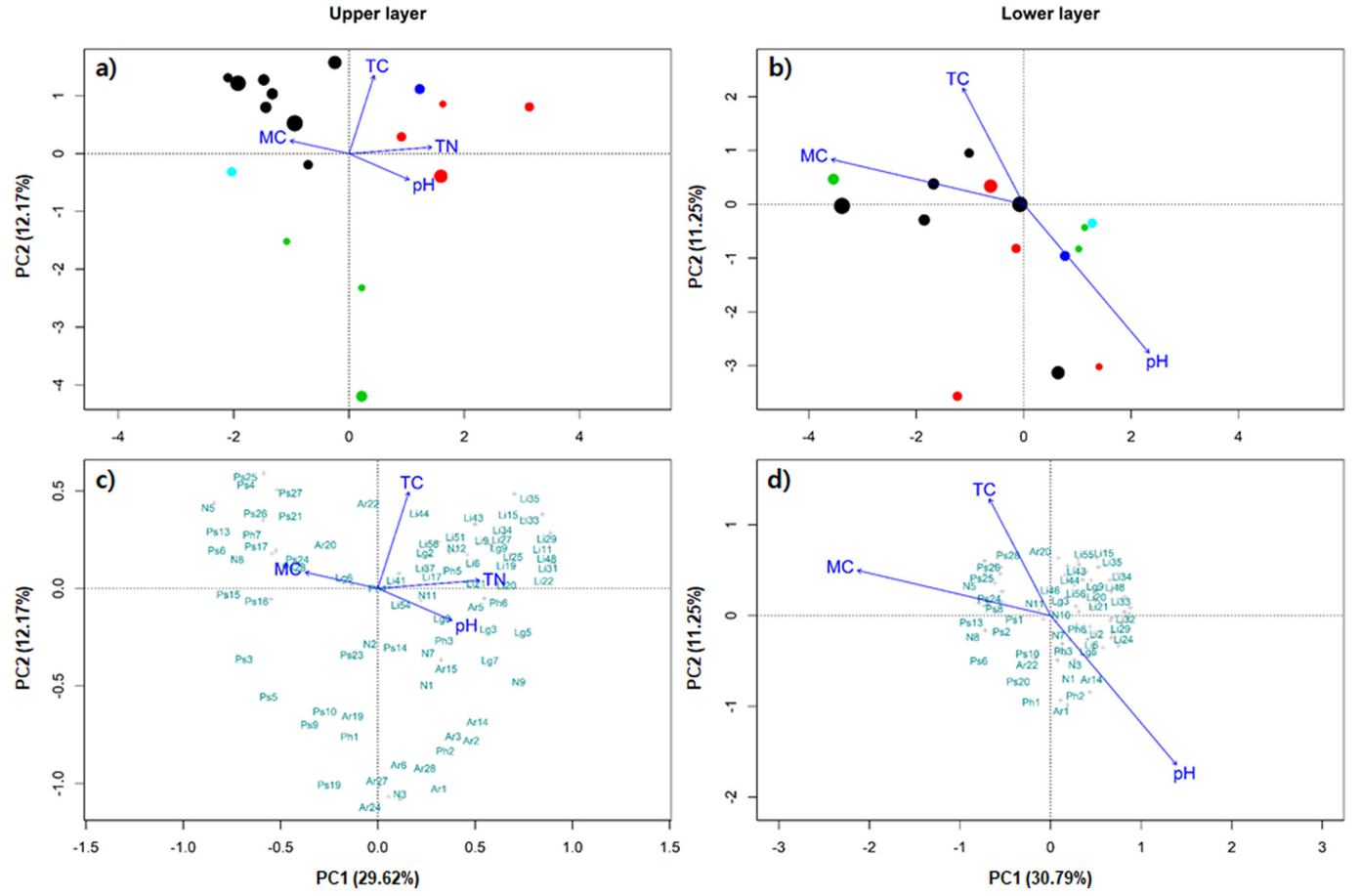

Fig. 4. Principal component analysis (PCA) biplots of the soil organic matter (SOM) compositional data for the Council, AK site. Both biplots showed the SOM composition, sampling sites, and main important soil variables: a) and c) in the upper soil layer and b) and d) in the lower soil layer. The significant soil physicochemical parameters are overlaid as arrows onto the ordination space (pH, MC, TC, TN). The colors represent the four vegetation groups described (Blue = lichen group, Red = *Betula nana*, *Rubus chamaemorus*, *Carex* spp. group, Black = *Eriophorum vaginatum* group, and green = mosses (*Sphagnum* spp.) group). The ball diameter in a biplot represents the PCNM1 correlation, i.e., the balls are spatially correlated with similar ones. Names of the variables are TC for total carbon content, TN for total nitrogen content, and MC for moisture content. (For interpretation of the references to color in this figure legend, the reader is referred to the web version of this article.)

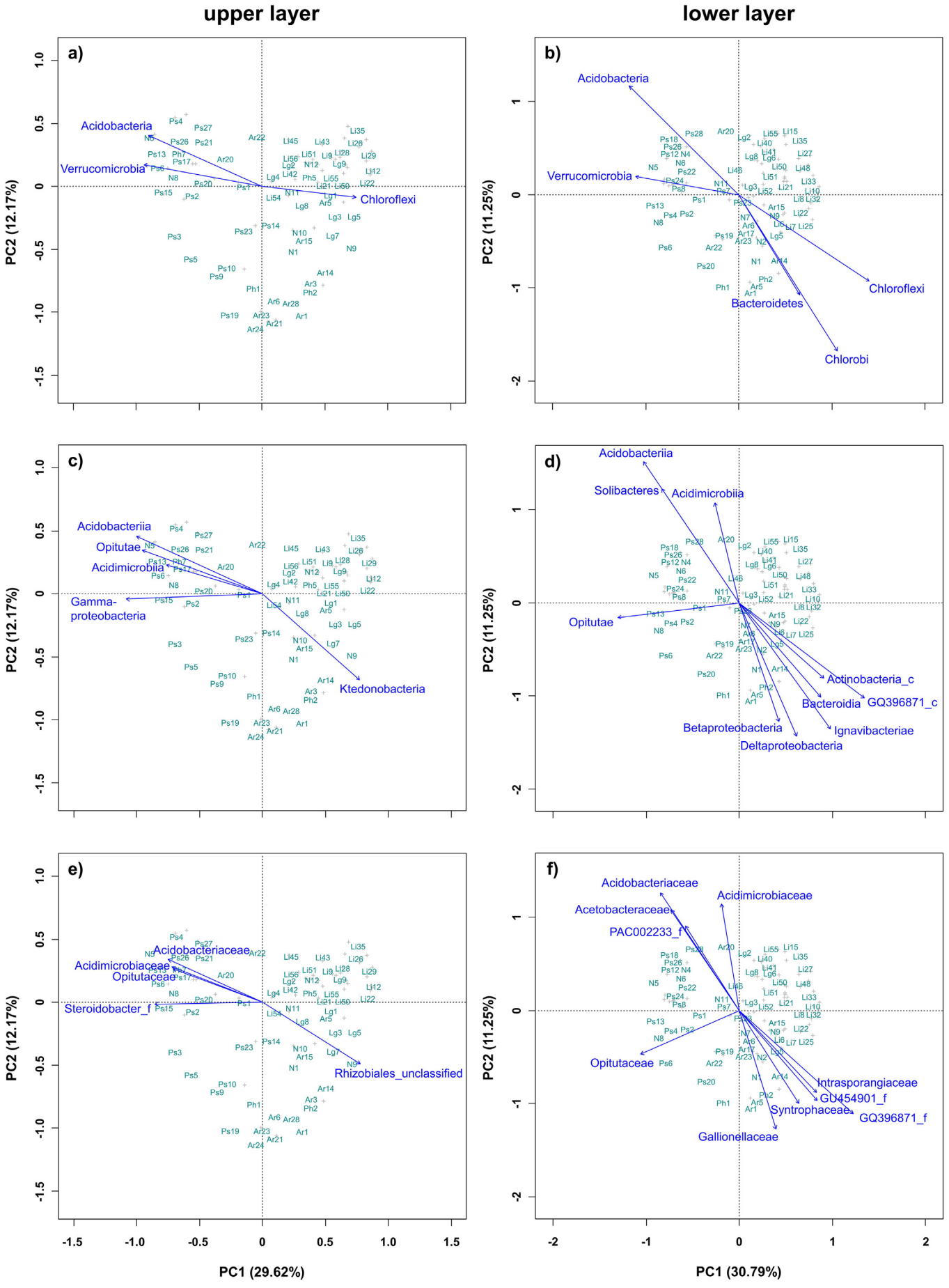
upper layer
lower layer
a)
b)
c)
d)
e)
f)
Acidobacteria
Verrucomicrobia
Chloroflexi
Bacteroidetes
Chlorobi
Acidobacteriia
Opitutae
Acidimicrobiia
Gamma-proteobacteria
Ktedonobacteria
Solibacteres
Actinobacteria_c
Bacteroidia
GQ396871_c
Betaproteobacteria
Ignavibacteriae
Deltaproteobacteria
Acidobacteriaceae
Acidimicrobiaceae
Opitutaceae
Steroidobacter_f
Rhizobiales_unclassified
Acetobacteraceae
PAC002233_f
Intrasporangiaceae
GU454901_f
Syntrophaceae
GQ396871_f
Gallionellaceae
PC1 (29.62%)
PC2 (12.17%)
PC1 (30.79%)
PC2 (11.25%)

upper and lower layers, respectively (Fig. 2) as suggested by hypothesis (3). When the upper soil layer was analyzed, we observed that the significant soil variables influencing overall SOM composition were pH ($F = 13.25$, $R^2 = 0.21$, p-value<0.001), MC ($F = 9.68$, $R^2 = 0.16$, p-value<0.001), TC ($F = 4.75$, $R^2 = 0.08$, p-value = 0.004), and TN ($F = 3.78$, $R^2 = 0.06$, p-value = 0.014). In the lower soil layer, the significant soil variables that influenced overall SOM composition were also MC ($F = 9.24$, $R^2 = 0.18$, p-value<0.001), pH ($F = 8.69$, $R^2 = 0.17$, p-value<0.001), and TC ($F = 3.59$, $R^2 = 0.07$, p-value = 0.026). The PCA ordination biplot, using both SOM composition and soil properties (Fig. 4), showed that the first axis in both layers was significantly correlated with MC (negative) and pH (positive), and that TN showed a positive correlation with PC1 in the upper layer. PC1 split the samples in both ordinations, placing those with higher pH or TN at the positive end and those with higher MC at the negative end (Fig. 4a, b). PC2 was significantly related to TC in both the upper and lower soil layers, and to pH in the lower soil layer; TC in both layers increased towards the positive end of PC2, while the pH in the lower layer increased towards the negative end.

3.6. Are there any relationships between SOM composition and bacterial community?

Soil bacteria were the second most important source of SOM composition variation, explaining 32% and 18% of the variation in the upper and lower layers, respectively (Fig. 2) as suggested by hypothesis (3). The overall SOM and bacterial community composition matrices showed significant correlations in both layers (mantel test r-statistic = 0.35 for the upper and 0.37 for the lower layer, p-values = 0.01). When the SOM composition in the upper layer was related to bacterial phyla, we observed that three phyla were significantly related to SOM compositional changes ($r^2 = 0.08$–0.36, Fig. 5a). Acidobacteria, and Verrucomicrobia increased towards the negative end of the first axis, and were related to polysaccharides and some aromatic compounds. Chloroflexi increased towards the positive end of the first axis and was related to lipids, N-containing compounds, and phenol compounds. In the lower layer, there were five bacterial phyla that were significantly related to SOM composition (Fig. 5b). Acidobacteria and Verrucomicrobia were negatively correlated with the first axis and were related to polysaccharides, while Bacteroidetes, Chlorobi, and Chloroflexi were negatively correlated with the second axis and were related to aromatic, N-containing and phenolic compounds.

The analysis of the relationship between SOM composition and bacterial family/class showed similar trends to that using bacterial phyla (Fig. 5). For example, Acidobacteria (Phylum)/Acidobacteriia (Class)/Acidobacteriaceae (Family) and Verrucomicrobia (Phylum)/Opitutae (Class)/Opitutaceae (Family) were negatively correlated with the first axis and were related to polysaccharides in both layers. Additionally, Chloroflexi (Phylum)/GQ396871_c (Class)/GQ396871_f (Family) and Bacteriodetes (Phylum) /Bacteroidia (Class)/GU454901_f (Family) were associated with aromatics, N-containing, and phenolic compounds in the lower layer. There were some bacterial classes/families that showed significant relationships with SOM composition despite showing no relationship at the phylum level. There were two cases of this in the upper layer: Acidimicrobiia (class)/Acidimicrobiaceae (family) and Gammaproteobacteria (class)/Steroidobacter_f (family) and four cases in the lower layer: Acidimicrobiia (class)/Acidimicrobiaceae (family), Actinobacteria_c (class)/Intrasporangiaceae (family), Deltaproteobacteria (class)/Syntrophaceae (family), and Betaproteobacteria (class)/Gallionellaceae (family).

4. Discussion

We used molecular techniques to reveal the inter-relationships between vegetation, bacterial community composition, soil properties, and SOM chemical composition in the acidic moist tussock tundra. The SOM at this study site was composed of polysaccharide-derived, lipid-derived, and aromatic compounds. The SOM compositional variation was explained well by the soil properties and bacterial community composition but did not reflect present vegetation composition. Soil pH, MC, and TC were the most significant variables that influenced SOM compositions. Bacterial community composition was the second most influential parameters explaining SOM compositional variation; while Acidobacteria and Verrucomicrobia were associated with polysaccharides, Chloroflexi was related to aromatic compounds.

4.1. SOM composition in the moist acidic tundra

The analysis of SOM characteristics showed that there were three different groups of sampling sites in both layers. The first group was located on the left-hand side of PC1 (Fig. 1c, d), included sites associated with polysaccharide-derived compounds, and was most associated with *Sphagnum* moss. *Sphagnum* species contain a significant amount of polysaccharide-pyrolysis products derived from hemicellulose cell walls (McClymont et al., 2011). Moreover, Treat et al. (2014) reported that *Sphagnum* moss peat comprises 55.8% of the polysaccharides in Alaskan tundra, and this ratio was similar to the average proportion of polysaccharides observed in this group of our soil samples. Furthermore, 4-isopropenylphenol (Ph7) was placed in the middle of the polysaccharides compounds in the loading plot (Fig. 1c, d) and is known as a major biomarker of *Sphagnum* moss (Stankiewicz et al., 1997; Schellekens et al., 2009; McClymont et al., 2011). These characteristics indicate that the molecular compositions of SOM in this first group were mainly affected by *Sphagnum* moss.

The second group was located on the right-hand side of PC1 and included sites mainly related to lipid-derived compounds (Fig. 1c, d). The hydrocarbons could indicate the origin of these compounds, based on their chain length. While the long-chain hydrocarbons were considered to have originated from vascular plant waxes (Gagosian et al., 1987; Matsumoto et al., 1990), the short and mid-chain hydrocarbons were thought to predominantly derive from the microbial synthesis or degradation of longer chains by microorganisms (Buurman et al., 2007; Kuhn et al., 2010). Although there was no clear distinction between long- and short/mid-chain hydrocarbons in the upper layer, the long-chain hydrocarbons were positioned on the positive side of PC2 in the lower layer (Fig. 1c, d). Moreover, lignin, a common element in the cell walls of vascular plants, was situated in the same area as the long-chain hydrocarbons. Therefore, the SOM in these samples largely comprised vascular plant-derived materials. Many studies have shown that the relative abundance of short and mid-chain hydrocarbons increases in deeper or more decomposed soil layers (Kögel-Knabner, 2000; Buurman et al., 2007; Grandy and Neff, 2008). The sampling sites associated with short/mid-chain hydrocarbons were located close to the aromatic compound distribution in the lower layer (Fig. 1c, d). This implies that the SOM in these samples were largely microbially processed and not in a fresh state.

The third group was located on the negative side of PC2 and contained sites associated with aromatic compounds (Fig. 1c, d). These sites were also positioned close to the short/mid-chain hydrocarbons. Sollins et al. (1996) found that aromatics showed similar behavior to alkyls regarding SOM decomposition. Both fractions were considered relatively recalcitrant against microbial decay

Fig. 5. Principal component analysis (PCA) biplots showing soil organic matter (SOM) composition and the main important bacterial variables: a), c), and e) for the upper soil layer and b), d), and f) for the lower soil layer in the Council, AK sites. The significant bacterial parameters are overlaid as arrows onto the ordination space. The a) and b) biplots are at the phylum level; the c) and d) biplots are at the class level; and the e) and f) biplots are at the family level. Names of the variables are Ps: polysaccharides; N: nitrogen-containing compounds; Lg: lignins; Ph: phenols; Ar: aromatics; Li: lipids.

(Vancampenhout et al., 2010). The dominance of alkyl-aromatics, such as toluene and ethylbenzene, in the aromatic group also supported the idea that these sites were not in a fresh state. These compounds were ascribed to microbial metabolite material and proteins (Chiavari and Galletti, 1992; Schellekens et al., 2009).

4.2. Spatial variability of SOM composition

Our results showed that SOM composition had clear spatial variability trend at the local scale, despite the vegetation, bacterial community composition, and soil physicochemical properties showing no variability (Fig. S2), and this partially supported hypothesis (1). The spatial variability of the SOM composition was partially related to elevation, which means that SOM composition is influenced by microtopography. There are numerous studies showing spatial patterns in soil parameters, SOM stocks, plant communities, and soil biogeochemical processes related to microtopography (Burke et al., 1999; Lipson et al., 2012), because topographic variation directly influences the flow of water and solar energy. Catena is a critical concept for explaining the effects of topographic variations on several soil parameters (Seibert et al., 2007). Thus, it seems that microtopographic differences induce changes in several SOM input materials and degradation components (Biasi et al., 2005; Malhotra et al., 2018).

Here, only the SOM composition in both layers and the bacterial community composition in the lower layer showed spatial structuring (Fig. S2); however, the vegetation, which could be the main source of SOM in this system, did not show any such pattern. These results only supported hypothesis (2) in regard to bacterial community composition. One plausible explanation is that the spatial patterns of the SOM composition reflect a past vegetation structure. This is also supported by the lack of direct effect of vegetation composition on SOM composition (Fig. 2). Our study site is an acidic moist tussock tundra, an environment with the perfect conditions to preserve organic material for long periods. KOPRI (2016) reported that the age of the Oa layer (23–30 cm depth) in the same site was more than 2000 BP according to radiocarbon dating. Thus, the spatial variability of the SOM composition might not be explained by the current status of the vegetation in acidic moist tundra soil. The history of soil development, past vegetation structure, or other historical parameters might have more explanatory power over the current spatial variability of the SOM composition.

4.3. Explanatory variables for SOM composition

4.3.1. Relationship between SOM composition and soil properties

Soil properties were the most influential factors for SOM compositional variance in both soil layers, supporting the idea that SOM formation and decomposition processes are mainly dependent on soil characteristics (Grandy and Neff, 2008; Kallenbach et al., 2016). Among the measured variables, soil pH, MC, and TC content showed highly significant relationships with SOM composition in both soil layers. The positive (soil pH) and negative (MC) correlation with PC1 might be explained by the presence of *Sphagnum* moss peat in the soil materials, despite its relatively low coverage in the current vegetation composition. *Sphagnum* moss acidifies soil through its high cation exchange capacity and maintains a high soil moisture content (Gough et al., 2000). Moreover, the negative correlation between TN content and the first axis in the upper layer (Fig. 4) is also supported by the characteristics of SOM derived from *Sphagnum* moss, since the moss contains much lower N concentrations than other vascular plants (Aerts et al., 1999; Turetsky et al., 2008). Thus, a higher proportion of *Sphagnum* moss peat in the samples on the left-hand side of PC1 would be associated with a higher MC, lower soil pH, and lower TN content.

The positive correlation between PC2 and TC content in both layers could be explained by the degradability of SOM compounds along PC2. Most of the aromatic and phenolic compounds, known to be recalcitrant, were situated on the negative end of PC2. Aromatic and phenolic compounds are not easily degraded. Thus, they remain after decomposition and are associated with lower TC contents. In the lower layer, PC2 was also negatively associated with soil pH. This also supports a more degraded status, as soil pH increases as decomposition proceeds in moist acidic tundra (Kim et al., 2016).

4.3.2. Relationship between SOM composition and bacterial community

SOM chemistry interacts with the microorganisms that play a major role in decomposing organic compounds in the soil. Grandy et al. (2009) showed that fungal to bacterial ratios and extracellular enzyme activities were correlated with specific SOM compounds. Moni et al. (2015) showed the microbial community structure was significantly related to SOM quality characterized by ^{13}C NMR. Our study also found some correlations between bacterial community and SOM composition, with bacteria being the second most important factor affecting SOM compositional variation. While the phylum Acidobacteria including several oligotrophic species could play a role of decomposing stable and recalcitrant SOM (Hale et al., 2019), it was also associated with high SOM contents (Li et al., 2018). Acidobacteria is also well known for its association with *Sphagnum* moss peat (Ivanova et al., 2016; Chroňáková et al., 2019), and this phylum was situated on the upper, left-hand side of PC1, an area which represented the characteristics of *Sphagnum*-derived SOM. In our study, Acidobacteriaceae was also associated with several polysaccharides in both layers, under conditions of higher moisture and carbon contents. This may be related to their ecological function of degrading cellulose under anaerobic conditions, which could lead to methane production (Schmidt et al., 2015). It was reported that the distribution of Acidobacteria and Verrucomicrobia were strongly associated with vegetation and soil organic carbon at different locations in landscape (Semenov et al., 2019). In our study, both phyla were positively associated with polysaccharide compounds including 4-isopropenylphenol (Ph7), a major biomarker of *Sphagnum* moss. The phylum Verrucomicrobia is also commonly observed in *Sphagnum* moss peat (Ivanova et al., 2016; Chroňáková et al., 2019). Although Verrucomicrobia is known as an oligotrophic group, its abundance was often high in carbon-rich horizons (Semenov et al., 2018). The spatial distribution of this phylum was associated with carbon dynamics (Fierer et al., 2013). Tveit et al. (2013) showed that Verrucomicrobia played an important role in plant polymer hydrolysis in high-Arctic peat soil. The Opitutaceae family was also located in the same area of the PCA plot as Acidobacteriaceae and could play a role in metabolizing carbohydrates which are important substrates for methanogenesis in anaerobic conditions (Tveit et al., 2015). Although Betaproteobacteria has been classified as a copiotrophic group (Ho et al., 2017), they could play a role in the degradation of recalcitrant aromatic compounds (Sperfeld et al., 2018), and our results show that they were associated with aromatic and phenolic compounds in both soil layers. However, at the family level, there were no Betaproteobacteria families associated with phenolic or aromatic compounds in the upper layer. Only the Gallionellaceae family was significantly related to these recalcitrant compounds in the lower layer. The Gallionellaceae family grew in acidic to neutral pHs, showing a negative correlation with pH (Trias et al., 2017) and has been studied as an aliphatic compound degrader (Muthukumar et al., 2003). Among the Gammaproteobacteria, the Steroidobacter_f family, was closely associated with polysaccharides in both layers. It was previously reported that a Steroidobacter strain could degrade the complex polysaccharides in rhizosphere and even agar materials (Sakai et al., 2014). The phylum Chlorflexi was linked to recalcitrant compounds such as aromatics, N-containing and phenolic compounds (Fig. 5). This result was consistent with the study of Duan et al. (2021) which showed a close correlation between Chloroflexi and aromaticity within macroaggregates. This might be related with the fraction of Chloroflexi increasing with depth (Tveit et al., 2015).

Many studies have emphasized the relationship between microbial community and the amount of organic matter or TC content, but its relationship with the chemical composition of organic matter in the field

has not received much attention. Even the utilization of organic matter by particular microbes has mainly been reported following substrate degradation tests using isolates in the laboratory. While we found some supportive results in laboratory experiments for the correlation between SOM characteristics and bacterial community in the field, some results were different from those of laboratory experiments. This requires further study to reveal whether particular bacterial groups prefer any specific pools of organic substrates or if specific bacterial guilds are needed for the degradation of specific compounds.

The evidence reported here, based on SOM pyrolysis products, suggests that our acidic moist tussock tundra soil samples can be grouped into polysaccharide-derived compounds, lipid-derived compounds, and aromatic compounds, showing that these three groups of sites have different sources of SOM formation or different degradation status. Interestingly, present vegetation composition was not a main factor in explaining SOM compositional variation under low temperature and high soil moisture conditions. Here, soil properties and bacterial community were the main variables explaining SOM compositional variation at a local scale. Thus, it seems that, at a local scale, soil abiotic and biotic processes are the most important factors shaping SOM composition in acidic moist tussock tundra, with a residual effect of actual vegetation as the source of organic matter. Moreover, we have described the inter-relationships among soil properties, bacterial community structure, and SOM composition comprehensively, using molecular approaches and a field-based study. This emphasizes the necessity of studying SOM composition in addition to the quantity of SOM, which is considered one of the most important variables related to bacterial community in most studies. Lastly, it should be noted that 46–70% of the variance in SOM composition at a local scale was unexplained by our measured variables. More studies are needed to reveal the important variables affecting SOM composition, so that we can satisfactorily understand SOM dynamics, decomposition, and stabilization processes through the characterization of SOM dimensionality.

CRediT authorship contribution statement

Sungjin Nam: Investigation, Formal analysis, Visualization, Writing – Original Draft, Review & Editing.

Josu G. Alday: Formal analysis, Visualization, Writing – Original Draft, Review & Editing.

Mincheol Kim: Investigation, Writing– Original Draft, Review & Editing, Funding acquisition.

Hyemin Kim: Investigation, Formal analysis, Writing - Review & Editing.

Yongkang Kim: Formal analysis, Writing - Review & Editing.

Taesung Park: Formal analysis, Writing - Review & Editing.

Hyoun Soo Lim: Investigation, Writing - Review & Editing.

Bang Yong Lee: Writing - Review & Editing, Funding acquisition.

Yoo Kyung Lee: Writing - Review & Editing, Supervision.

Ji Young Jung: Methodology, Writing – Original Draft, Review & Editing, Conceptualization.

Declaration of competing interest

The authors declare that they have no known competing financial interests or personal relationships that could have appeared to influence the work reported in this paper.

Acknowledgments

This study was supported by the National Research Foundation of Korea funded by the Korean Government [NRF-2016M1A5A1901770, PN17082] and [NRF-2016M1A5A1901769, PN20081]. J.G.A. was supported by Ramon y Cajal fellowship (RYC-2016-20528). Fieldwork permits were granted by the UAF. We are thankful to Prof. Jaeweon Cho at Ulsan National Institute of Science and Technology (UNIST) for allowing us to use a pyrolyzer and GC/MS, to Dr. Chien-Lu Ping for interpreting Alaskan soil feature in this site, and to Ms. Jane Lee for her help in English editing.

Appendix A. Supplementary data

Supplementary data to this article can be found online at https://doi.org/10.1016/j.scitotenv.2021.145386.

References

Aerts, R., Verhoeven, J.T.A., Whigham, D.F., 1999. Plant-mediated controls on nutrient cycling in temperate fens and bogs. Ecology 80, 2170–2181.

Biasi, C., Wanek, W., Rusalimova, O., Kaiser, C., Meyer, H., Barsukov, P., Richter, A., 2005. Microtopography and plant-cover controls on nitrogen dynamics in hummock tundra ecosystems in Siberia. Arct. Antarct. Alp. Res. 37, 435–443.

Burke, I.C., Lauenroth, W.K., Riggle, R., Brannen, P., Madigan, B., Beard, S., 1999. Spatial variability of soil properties in the shortgrass steppe: the relative importance of topography, grazing, microsite, and plant species in controlling spatial patterns. Ecosystems 2, 422–438.

Buurman, P., Peterse, F., Martin, G.A., 2007. Soil organic matter chemistry in allophanic soils: a pyrolysis-GC/MS study of a Costa Rican Andosol catena. Eur. J. Soil Sci. 58, 1330–1347.

Chefetz, B., Tarchitzky, J., Deshmukh, A.P., Hatcher, P.G., Chen, Y., 2002. Structural characterization of soil organic matter and humic acids in particle-size fractions of an agricultural soil. Soil Sci. Soc. Am. J. 66, 129–141.

Chen, H., Blosser, G.D., Majidzadeh, H., Liu, X., Conner, W.H., Chow, A.T., 2018. Integration of an automated identification-quantification pipeline and statistical techniques for pyrolysis GC/MS tracking of the molecular fingerprints of natural organic matter. J. Anal. Appl. Pyrolysis 134, 371–380.

Chiavari, G., Galletti, G.C., 1992. Pyrolysis-gas chromatography/mass spectrometry of amino acids. J. Anal. Appl. Pyrolysis 24, 123–137.

Dai, X.Y., Ping, C.L., Michaelson, G.J., 2002. Characterizing soil organic matter in Arctic tundra soils by different analytical approaches. Org. Geochem. 33, 407–419.

Davidson, E.A., Janssens, I.A., 2006. Temperature sensitivity of soil carbon decomposition and feedbacks to climate change. Nature 440, 165–173.

De la Rosa, J.M., Jimenez-Morillo, N.T., Gonzalez-Perez, J.A., Almendros, G., Vieira, D., Knicker, H.E., Keizer, J., 2019. Mulching-induced preservation of soil organic matter quality in a burnt eucalypt plantation in central Portugal. J. Environ. Manag. 231, 1135–1144.

Derenne, S., Quenea, K., 2015. Analytical pyrolysis as a tool to probe soil organic matter. J. Anal. Appl. Pyrolysis 111, 108–120.

Derenne, S., Tu, T.T.N., 2014. Characterizing the molecular structure of organic matter from natural environments: an analytical challenge. Compt. Rendus Geosci. 346, 53–63.

Ding, G., Novak, J.M., Amarasiriwardena, D., Hunt, P.G., Xing, B.S., 2002. Soil organic matter characteristics as affected by tillage management. Soil Sci. Soc. Am. J. 66, 421–429.

Duan, Y., Chen, L., Zhang, J., Li, D., Han, X., Zhu, B., Li, Y., Zhao, B., Huang, P., 2021. Long-term fertilisation reveals close associations between soil organic carbon composition and microbial traits at aggregate scales. Agric. Ecosyst. Environ. 306.

Fierer, N., Ladau, J., Clemente, J.C., Leff, J.W., Owens, S.M., Pollard, K.S., Knight, R., Gilbert, J.A., McCulley, R.L., 2013. Reconstructing the microbial diversity and function of pre-agricultural tallgrass prairie soils in the United States. Science 342, 621.

Gagosian, R.B., Peltzer, E.T., Merrill, J.T., 1987. Long-range transport of terrestrially derived lipids in aerosols from the South-Pacific. Nature 325, 800–804.

Gleixner, G., Poirier, N., Bol, R., Balesdent, J., 2002. Molecular dynamics of organic matter in a cultivated soil. Org. Geochem. 33, 357–366.

González-Pérez, J.A., Arbelo, C.D., González-Vila, F.J., Rodríguez, A.R., Almendros, G., Armas, C.M., Polvillo, O., 2007. Molecular features of organic matter in diagnostic horizons from andosols as seen by analytical pyrolysis. J. Anal. Appl. Pyrolysis 80, 369–382.

Gough, L., Shaver, G.R., Carroll, J., Royer, D.L., Laundre, J.A., 2000. Vascular plant species richness in Alaskan arctic tundra: the importance of soil pH. J. Ecol. 88, 54–66.

Grandy, A.S., Neff, J.C., 2008. Molecular C dynamics downstream: the biochemical decomposition sequence and its impact on soil organic matter structure and function. Sci. Total Environ. 404, 297–307.

Grandy, A.S., Strickland, M.S., Lauber, C.L., Bradford, M.A., Fierer, N., 2009. The influence of microbial communities, management, and soil texture on soil organic matter chemistry. Geoderma 150, 278–286.

Guo, X.P., Meng, M.J., Zhang, J.C., Chen, H.Y.H., 2016. Vegetation change impacts on soil organic carbon chemical composition in subtropical forests. Sci. Rep. 6, 29607.

Hale, L., Feng, W., Yin, H., Guo, X., Zhou, X., Bracho, R., Pegoraro, E., Penton, C.R., Wu, L., Cole, J., Konstantinidis, K.T., Luo, Y., Tiedje, J.M., Schuur, E.A.G., Zhou, J., 2019. Tundra microbial community taxa and traits predict decomposition parameters of stable, old soil organic carbon. ISME J. 13, 2901–2915.

Chroňáková, A., Bárta, J., Kaštovská, E., Urbanová, Z., Picek, T., 2019. Spatial heterogeneity of belowground microbial communities linked to peatland microhabitats with different plant dominants. FEMS Microbiol. Ecol. 95, fiz130.

Ho, A., Di Lonardo, D.P., Bodelier, P.L., 2017. Revisiting life strategy concepts in environmental microbial ecology. FEMS Microbiol. Ecol. 93, fix006.
Hugelius, G., Strauss, J., Zubrzycki, S., Harden, J.W., Schuur, E.A.G., Ping, C.L., Schirrmeister, L., Grosse, G., Michaelson, G.J., Koven, C.D., O'Donnell, J.A., Elberling, B., Mishra, U., Camill, P., Yu, Z., Palmtag, J., Kuhry, P., 2014. Estimated stocks of circumpolar permafrost carbon with quantified uncertainty ranges and identified data gaps. Biogeosciences 11, 6573–6593.
Ivanova, A.A., Wegner, C.E., Kim, Y., Liesack, W., Dedysh, S.N., 2016. Identification of microbial populations driving biopolymer degradation in acidic peatlands by metatranscriptomic analysis. Mol. Ecol. 25, 4818–4835.
Jimenez-Gonzalez, M.A., De la Rosa, J.M., Jimenez-Morillo, N.T., Almendros, G., Gonzalez-Perez, J.A., Knicker, H., 2016. Post-fire recovery of soil organic matter in a Cambisol from typical Mediterranean forest in Southwestern Spain. Sci. Total Environ. 572, 1414–1421.
Jimenez-Morillo, N.T., Almendros, G., De la Rosa, J.M., Jordan, A., Zavala, L.M., Granged, A.J.P., Gonzalez-Perez, J.A., 2020. Effect of a wildfire and of post-fire restoration actions in the organic matter structure in soil fractions. Sci. Total Environ. 728, 138715.
Kallenbach, C.M., Frey, S.D., Grandy, A.S., 2016. Direct evidence for microbial-derived soil organic matter formation and its ecophysiological controls. Nat. Commun. 7, 13630.
Karhu, K., Auffret, M.D., Dungait, J.A.J., Hopkins, D.W., Prosser, J.I., Singh, B.K., Subke, J.A., Wookey, P.A., Ågren, G.I., Sebastià, M.T., Gouriveau, F., Bergkvist, G., Meir, P., Nottingham, A.T., Salinas, N., Hartley, I.P., 2014. Temperature sensitivity of soil respiration rates enhanced by microbial community response. Nature 513, 81–84.
Kim, H.M., Jung, J.Y., Yergeau, E., Hwang, C.Y., Hinzman, L., Nam, S., Hong, S.G., Kim, O.S., Chun, J., Lee, Y.K., 2014. Bacterial community structure and soil properties of a subarctic tundra soil in Council, Alaska. FEMS Microbiol. Ecol. 89, 465–475.
Kim, H.M., Lee, M.J., Jung, J.Y., Hwang, C.Y., Kim, M., Ro, H.M., Chun, J., Lee, Y.K., 2016. Vertical distribution of bacterial community is associated with the degree of soil organic matter decomposition in the active layer of moist acidic tundra. J. Microbiol. 54, 713–723.
Klein, K., Gross-Schmölders, M., De la Rosa, J.M., Alewell, C., Leifeld, J., 2020. Investigating the influence of instrumental parameters and chemical composition on pyrolysis efficiency of peat. Commun. Soil Sci. Plant Anal. 51, 1572–1581.
Kögel-Knabner, I., 2000. Analytical approaches for characterizing soil organic matter. Org. Geochem. 31, 609–625.
KOPRI, 2016. Establishment of Circum Arctic Permafrost Environment Change Monitoring Network and Future Prediction Techniques: CAPEC Project. In: Lee, B.Y. (Ed.), Ministry of Science. Republic of Korea, ICT and Future Planning, pp. 540–541.
Kuhn, T.K., Krull, E.S., Bowater, A., Grice, K., Gleixner, G., 2010. The occurrence of short chain n-alkanes with an even over odd predominance in higher plants and soils. Org. Geochem. 41, 88–95.
Lal, R., 2004. Soil carbon sequestration impacts on global climate change and food security. Science 304, 1623–1627.
Legendre, P., Legendre, L., 2012. Numerical Ecology, Volume 24. 3rd edition. Elsevier.
Li, D., Chen, L., Xu, J., Ma, L., Olk, D.C., Zhao, B., Zhang, J., Xin, X., 2018. Chemical nature of soil organic carbon under different long-term fertilization regimes is coupled with changes in the bacterial community composition in a Calcaric Fluvisol. Biol. Fertil. Soils 54, 999–1012.
Lipson, D.A., Zona, D., Raab, T.K., Bozzolo, F., Mauritz, M., Oechel, W.C., 2012. Water-table height and microtopography control biogeochemical cycling in an Arctic coastal tundra ecosystem. Biogeosciences 9, 577–591.
López-Martin, M., Velasco-Molina, M., Knicker, H., 2016. Variability of the quality and quantity of organic matter in soil affected by multiple wildfires. J. Soils Sediments 16, 360–370.
Lv, G.J., Wu, S.B., 2012. Analytical pyrolysis studies of corn stalk and its three main components by TG-MS and Py-GC/MS. J. Anal. Appl. Pyrolysis 97, 11–18.
Malhotra, A., Moore, T.R., Limpens, J., Roulet, N.T., 2018. Post-thaw variability in litter decomposition best explained by microtopography at an ice-rich permafrost peatland. Arct. Antarct. Alp. Res. 50, e1415622.
Mambelli, S., Bird, J.A., Gleixner, G., Dawson, T.E., Torn, M.S., 2011. Relative contribution of foliar and fine root pine litter to the molecular composition of soil organic matter after in situ degradation. Org. Geochem. 42, 1099–1108.
Matsumoto, G.I., Akiyama, M., Watanuki, K., Torii, T., 1990. Unusual distributions of long-chain normal-alkanes and n-alkenes in Antarctic soil. Org. Geochem. 15, 403–412.
McClymont, E.L., Bingham, E.M., Nott, C.J., Chambers, F.M., Pancost, R.D., Evershed, R.P., 2011. Pyrolysis GC-MS as a rapid screening tool for determination of peat-forming plant composition in cores from ombrotrophic peat. Org. Geochem. 42, 1420–1435.
Meersmans, J., De Ridder, F., Canters, F., De Baets, S., Van Molle, M., 2008. A multiple regression approach to assess the spatial distribution of soil organic carbon (SOC) at the regional scale (Flanders, Belgium). Geoderma 143, 1–13.
Mehrabanian, M., 2013. Molecular geochemistry of soil organic matter by pyrolysis gas chromatograpy/mass spectrometry (GC/MS) technique: a review. J. Soil Sci. Manage. 4, 11–16.
Moni, C., Lerch, T.Z., Knoth de Zarruk, K., Strand, L.T., Forte, C., Certini, G., Rasse, D.P., 2015. Temperature response of soil organic matter mineralisation in arctic soil profiles. Soil Biol. Biochem. 88, 236–246.
Moorhead, D.L., Sinsabaugh, R.L., 2006. A theoretical model of litter decay and microbial interaction. Ecol. Monogr. 76, 151–174.
Muthukumar, N., Mohanan, S., Maruthamuthu, S., Subramanian, N., Palaniswamy, M.R., 2003. Role of Brucella sp. and Gallionella sp. in oil degradation and corrosion. Electrochem. Commun. 5, 421–425.
Oksanen, J., Blanchet, F.G., Kindt, R., Legendre, P., Minchin, P.R., O'Hara, R.B., Simpson, G.L., Solymos, P., Henry, M., Stevens, H. and Wagner, H., 2019. Vegan: community ecology package. R-package version 2.3–0. Available at: http://cran.r-project.org/package=vegan.
Park, J.S., Lee, E.J., 2014. Geostatistical analyses and spatial distribution patterns of tundra vegetation in Council, Alaska. J. Eco. Env. 37, 53–60.
Pisani, O., Lin, L.H., Lun, O.O.Y., Lajtha, K., Nadelhoffer, K.J., Simpson, A.J., Simpson, M.J., 2016. Long-term doubling of litter inputs accelerates soil organic matter degradation and reduces soil carbon stocks. Biogeochemistry 127, 1–14.
Post, W.M., Kwon, K.C., 2000. Soil carbon sequestration and land-use change: processes and potential. Glob. Chang. Biol. 6, 317–327.
R Core Team, 2020. R: A language and environment for statistical computing. R Foundation for Statistical Computing, Vienna, Austria https://www.R-project.org/.
Saiz-jimenez, C., 1994. Analytical pyrolysis of humic substances: pitfalls, limitations, and possible solutions. Environ. Sci. Technol. 28, 1773–1780.
Sakai, M., Hosoda, A., Ogura, K., Ikenaga, M., 2014. The growth of Steroidobacter agariperforans sp. nov., a novel agar-degrading bacterium isolated from soil, is enhanced by the diffusible metabolites produced by bacteria belonging to Rhizobiales. Microbes Environ. 29, 89–95.
Schellekens, J., Buurman, P., Pontevedra-Pombal, X., 2009. Selecting parameters for the environmental interpretation of peat molecular chemistry - a pyrolysis-GC/MS study. Org. Geochem. 40, 678–691.
Schellekens, J., Almeida-Santos, T., Macedo, R.S., Buurman, P., Kuyper, T.W., Vidal-Torrado, P., 2017. Molecular composition of several soil organic matter fractions from anthropogenic black soils (Terra Preta de Índio) in Amazonia – a pyrolysis-GC/MS study. Geoderma 288, 154–165.
Schloss, P.D., Westcott, S.L., Ryabin, T., Hall, J.R., Hartmann, M., Hollister, E.B., Lesniewski, R.A., Oakley, B.B., Parks, D.H., Robinson, C.J., Sahl, J.W., Stres, B., Thallinger, G.G., Van Horn, D.J., Weber, C.F., 2009. Introducing mothur: open-source, platform-independent, community-supported software for describing and comparing microbial communities. Appl. Environ. Microbiol. 759, 7537–7541.
Schmidt, M.W.I., Torn, M.S., Abiven, S., Dittmar, T., Guggenberger, G., Janssens, I.A., Kleber, M., Kögel-Knabner, I., Lehmann, J., Manning, D.A.C., Nannipieri, P., Rasse, D.P., Weiner, S., Trumbore, S.E., 2011. Persistence of soil organic matter as an ecosystem property. Nature 478, 49–56.
Schmidt, O., Horn, M.A., Kolb, S., Drake, H.L., 2015. Temperature impacts differentially on the methanogenic food web of cellulose-supplemented peatland soil. Environ. Microbiol. 17, 720–734.
Schuur, E.A.G., Bockheim, J., Canadell, J.G., Euskirchen, E., Field, C.B., Goryachkin, S.V., Hagemann, S., Kuhry, P., Lafleur, P.M., Lee, H., Mazhitova, G., Nelson, F.E., Rinke, A., Romanovsky, V.E., Shiklomanov, N., Tarnocai, C., Venevsky, S., Vogel, J.G., Zimov, S.A., 2008. Vulnerability of permafrost carbon to climate change: implications for the global carbon cycle. Bioscience 58, 701–714.
Schuur, E.A.G., Vogel, J.G., Crummer, K.G., Lee, H., Sickman, J.O., Osterkamp, T.E., 2009. The effect of permafrost thaw on old carbon release and net carbon exchange from tundra. Nature 459, 556–559.
Seibert, J., Stendahl, J., Sørensen, R., 2007. Topographical influences on soil properties in boreal forests. Geoderma 141, 139–148.
Semenov, M.V., Chernov, T.I., Tkhakakhova, A.K., Zhelezova, A.D., Ivanova, E.A., Kolganova, T.V., Kutovaya, O.V., 2018. Distribution of prokaryotic communities throughout the Chernozem profiles under different land uses for over a century. Appl. Soil Ecol. 127, 8–18.
Semenov, M.V., Manucharova, N.A., Krasnov, G.S., Nikitin, D.A., Stepanov, A.L., 2019. Biomass and taxonomic structure of microbial communities in soils of the right-bank basin of the Oka River. Eurasian J. Soil Sci. 52, 971–981.
Sollins, P., Homann, P., Caldwell, B.A., 1996. Stabilization and destabilization of soil organic matter: mechanisms and controls. Geoderma 74, 65–105.
Sperfeld, M., Rauschenbach, C., Diekert, G., Studenik, S., 2018. Microbial community of a gasworks aquifer and identification of nitrate-reducing Azoarcus and Georgfuchsia as key players in BTEX degradation. Water Res. 132, 146–157.
Stankiewicz, B.A., Hutchins, J.C., Thomson, R., Briggs, D.E.G., Evershed, R.P., 1997. Assessment of bog-body tissue preservation by pyrolysis gas chromatography/mass spectrometry. Rapid Commun. Mass Spectrom. 11, 1884–1890.
Stewart, C.E., 2012. Evaluation of angiosperm and fern contributions to soil organic matter using two methods of pyrolysis-gas chromatography-mass spectrometry. Plant Soil 351, 31–46.
Stewart, C.E., Neff, J.C., Amatangelo, K.L., Vitousek, P.M., 2011. Vegetation effects on soil organic matter chemistry of aggregate fractions in a Hawaiian forest. Ecosystems 14, 382–397.
Treat, C.C., Wollheim, W.M., Varner, R.K., Grandy, A.S., Talbot, J., Frolking, S., 2014. Temperature and peat type control CO_2 and CH_4 production in Alaskan permafrost peats. Glob. Chang. Biol. 20, 2674–2686.
Trias, R., Menez, B., le Campion, P., Zivanovic, Y., Lecourt, L., Lecoeuvre, A., Schmitt-Kopplin, P., Uhl, J., Gislason, S.R., Alfreethsson, H.A., Mesfin, K.G., Snaebjornsdottir, S.O., Aradottir, E.S., Gunnarsson, I., Matter, J.M., Stute, M., Oelkers, E.H., Gerard, E., 2017. High reactivity of deep biota under anthropogenic CO2 injection into basalt. Nat. Commun. 8, 1063.
Turetsky, M.R., Crow, S.E., Evans, R.J., Vitt, D.H., Wieder, R.K., 2008. Trade-offs in resource allocation among moss species control decomposition in boreal peatlands. J. Ecol. 96, 1297–1305.
Tveit, A., Schwacke, R., Svenning, M.M., Urich, T., 2013. Organic carbon transformations in high-Arctic peat soils: key functions and microorganisms. ISME J. 7, 299–311.
Tveit, A.T., Urich, T., Frenzel, P., Svenning, M.M., 2015. Metabolic and trophic interactions modulate methane production by Arctic peat microbiota in response to warming. Proc. Natl. Acad. Sci. U. S. A. 112, E2507–E2516.

Vancampenhout, K., Wouters, K., De Vos, B., Buurman, P., Swennen, R., Deckers, J., 2009. Differences in chemical composition of soil organic matter in natural ecosystems from different climatic regions - a pyrolysis-GC/MS study. Soil Biol. Biochem. 41, 568–579.

Vancampenhout, K., De Vos, B., Wouters, K., Van Calster, H., Swennen, R., Buurman, P., Deckers, J., 2010. Determinants of soil organic matter chemistry in maritime temperate forest ecosystems. Soil Biol. Biochem. 42, 220–233.

Wang, T., Camps-Arbestain, M., Hedley, C., 2016. Factors influencing the molecular composition of soil organic matter in New Zealand grasslands. Agric. Ecosyst. Environ. 232, 290–301.

Yoon, S.H., Ha, S.M., Kwon, S., Lim, J., Kim, Y., Seo, H., Chun, J., 2017. Introducing EzBioCloud: a taxonomically united database of 16S rRNA gene sequences and whole-genome assemblies. Int. J. Syst. Evol. Microbiol. 67, 1613–1617.